Estuaries and Coasts (2022) 45:2414–2427
https://doi.org/10.1007/s12237-022-01112-7

Tidal Freshwater Zones Modify the Forms and Timing of Nitrogen Export from Rivers to Estuaries

Hengchen Wei[1,2] · Xin Xu[2] · Allan E. Jones[3] · Amber K. Hardison[4] · Kevan B. Moffett[5] · James W. McClelland[2]

Received: 5 February 2022 / Revised: 30 June 2022 / Accepted: 28 July 2022 / Published online: 8 August 2022

Abstract

It is widely recognized that nitrogen (N) inputs from watersheds to estuaries are modified during transport through river networks, but changes within tidal freshwater zones (TFZs) have been largely overlooked. This paper sheds new light on the role that TFZs play in modifying the timing and forms of N inputs to estuaries by (1) characterizing spatial and temporal variability of N concentrations and forms in the TFZs of the Mission and Aransas rivers, Texas, USA, and (2) examining seasonal fluxes of N into and out of the Aransas River TFZ. Median concentrations of dissolved inorganic N (DIN) were lower in the TFZs than in upstream non-tidal river reaches and exhibited spatial gradients linked to locations of major N inputs. These spatial patterns were stronger during winter than summer. The forms of N also changed substantially, with DIN changing to organic N (primarily phytoplankton) within the TFZs. Discharge and N flux comparisons for the Aransas River TFZ demonstrated that secular tidal patterns modulate the timing of N export during baseflow conditions: N export far exceeded input during winter, whereas export and input were relatively balanced during summer. While more data are needed to build an annual N budget, our results show that TFZ can change the timing and form of N export immediately upstream of estuaries.

Keywords Tidal freshwater zone · Nitrogen · Eutrophication · Phytoplankton · Denitrification

Introduction

Coastal ecosystems are deteriorating globally due to human activities (Lotze 2006; Worm et al. 2006; Halpern et al. 2008). Eutrophication is one of the most severe issues threatening these ecosystems, causing problems such as harmful algal blooms, decreased water clarity, loss of seagrass beds, altered food webs, and hypoxia (Cloern 2001; Smith and Schindler 2009). Coastal eutrophication has worsened throughout the twentieth and twenty-first centuries, largely due to increases in anthropogenic nitrogen (N) fixation to support growing agricultural and population demands (Boesch 2002).

Effective management of coastal eutrophication requires improved understanding of N transformations and losses/gains during transport along river networks. While the importance of headwater streams in removing watershed-derived N is widely recognized (Peterson 2001), transformations and removal/production can also be substantial in the lower reaches of rivers (Wollheim et al. 2006; Tank et al. 2008). Indeed, Seitzinger et al. (2002) estimated that half of N retention during transit through river networks may occur within the last 10% of the total stream length. This disproportionately high retention in lower river reaches highlights the importance of processes occurring near the river-estuary interface, where tidal energy can cause widened channels and slowed-down, or even reversed flow (Ensign et al. 2013).

Tidal effects on river flow often reach farther inland than saline waters from the ocean, resulting in tidal freshwater zones (TFZs) of varying extent and persistence (Mooney and McClelland 2012; Jones et al. 2019). TFZs have been

Communicated by Lijun Hou

✉ Hengchen Wei
Hengchen_wei@163.com

[1] School of Environmental Science and Engineering, Nanjing Tech University, Nanjing 211816, China

[2] University of Texas Marine Science Institute, Port Aransas, TX, USA

[3] Illinois State Water Survey, University of Illinois, Champaign, IL, USA

[4] College of William & Mary, Virginia Institute of Marine Science, Gloucester Point, VA, USA

[5] School of the Environment, Washington State University, Vancouver, WA, USA

documented in many rivers worldwide, including smaller rivers such as the Hudson (Findlay et al. 1991), Potomac (Lovley and Phillips 1986), James (Bukaveckas and Isenberg 2013), Scheldt (Hellings et al. 1999), and Youngsan rivers (Sin et al. 2015), and larger rivers such as the Amazon (Nowacki et al. 2019), Mississippi (Amphlett and Brabben 1990), and Yangtze rivers (Guo et al. 2015). Indeed, tidal signals have been shown to propagate hundreds of kilometers inland in some of these rivers. TFZs are often associated with extensive intertidal marshes/forests, and a considerable amount of work has focused on sediment and nutrient source/sink dynamics within these intertidal wetland ecosystems (e.g., Conner et al. 2007; Ensign and Noe 2018; Megonigal and Neubauer 2019). Far less research on TFZs has addressed nutrient transformations and input/output fluxes in the river channels themselves.

Due to the complexity of their hydrodynamics, a broadly accepted definition for TFZs is lacking. In a study parallel to the current one, Jones et al. (2020) provided a framework to describe the physical extent of a TFZ, the upper boundary of which is defined by vertical tidal oscillations of water levels and the lower boundary of which is defined by salinity. According to this definition, the location and extent of a TFZ within a river-estuary continuum are dynamic, responding to variations in tidal forcing and rates of freshwater inflow (Ensign et al. 2013; Hoitink and Jay 2016; Jones et al. 2020). During extreme rain events, high river discharge can effectively turn TFZs into passive conduits that rapidly deliver watershed-derived nutrients to estuaries (Mooney and McClelland 2012; Bruesewitz et al. 2013). During baseflow conditions, TFZs may serve as important biogeochemical reactors with the potential to substantially alter watershed inputs to estuaries (Xu et al. 2021).

Although TFZs may be important conduits of nutrients to the coastline, N transport and transformations within TFZs are still not adequately understood (Arndt et al. 2011). Focused studies of nutrient cycling within TFZs have been conducted in the Hudson (Lampman et al. 1999), James (Bukaveckas and Isenberg 2013), Potomac (Jones et al. 2008), and Delaware (Lebo and Sharp 1993) rivers. Some broader studies of nutrient cycling in river networks have also explicitly recognized TFZs (Minaudo et al. 2016; Romero et al. 2016). However, TFZs are still not routinely recognized as distinct physical, chemical, or ecological components of the river-estuary continuum (Arndt et al. 2011; Ensign and Noe 2018; Jones et al. 2020).

With coastal areas worldwide experiencing increasing economic development, continued N fertilization, accelerated sea-level rise, and other impacts of climate change, improving our understanding of how TFZs modify N fluxes from land to sea is timely and critical to both scientific and environmental management communities. To examine N transport and transformations occurring within TFZs, we (1) characterized spatial and temporal variability of N forms and concentrations in the TFZs of the Mission River (MR) and Aransas River (AR) in Texas, USA, and (2) combined these data with previously published water flux/budget data (Jones et al. 2019) to examine seasonal (winter and summer) N inputs to and exports from the AR TFZ. We did not attempt to estimate N fluxes into and out of the MR TFZ because we did not have a complete, published water budget for that system. The AR and MR TFZs have very little fringing wetland vegetation. Thus, we were able to focus on in-channel nutrient dynamics without confounding effects related to tidal freshwater marshes/forests that dominate some other systems.

Methods

Study Area

The MR and AR watersheds are located on the coastal plain of south Texas (Fig. 1a inset), and both rivers are the primary freshwater sources to Copano Bay (Evans et al. 2012; Mooney and McClelland 2012). The local climate is semi-arid, with average annual evaporation (151.3 cm) exceeding average annual precipitation (88.6 cm), and the majority of annual precipitation is delivered in a few intense rainfall events each year (Evans et al. 2012). Municipal wastewater, however, is discharged into the rivers throughout the year and serves as a continuous source of water and anthropogenic nutrients to the rivers. The AR receives 14.4 million liters per day (mld) of effluent from 10 wastewater treatment plants (WWTPs) in its watershed. These WWTP inputs account for more than 80% of the water in the AR during baseflow periods (Mooney and McClelland 2012). The MR receives 2.63 mld of effluent from 4 WWTPs (Mooney and McClelland 2012); one of these WWTPs discharges (0.73 mld) laterally into the MR TFZ via Dry Creek (Fig. 1b).

Average daily tidal fluctuations in the study region are small (~ 0.15 m), but mean tidal levels vary much more on an annual scale. For example, in 2016, the difference between the maximum and minimum tide levels in Copano Bay was ~ 1 m (monitored by the National Oceanic and Atmospheric Administration (NOAA) at tide gage 8,774,770 at Rockport, Texas; https://tidesandcurrents.noaa.gov). This broader tidal range at an annual scale is due to semiannual secular tidal variations (Ward 1997).

The MR and AR TFZs, physically defined using a combination of water level, flow, and electrical conductivity (salinity) data, span ~ 15 km and 55 km respectively in the lower reaches of the two rivers (Jones 2017; Jones et al. 2020). Sampling stations were established at five locations along the MR (MR1 – MR5, Fig. 1b) and six locations along the AR (AR0–AR5, Fig. 1b). MR1 and AR0 were non-tidal stations near the upper boundaries of the TFZs, which

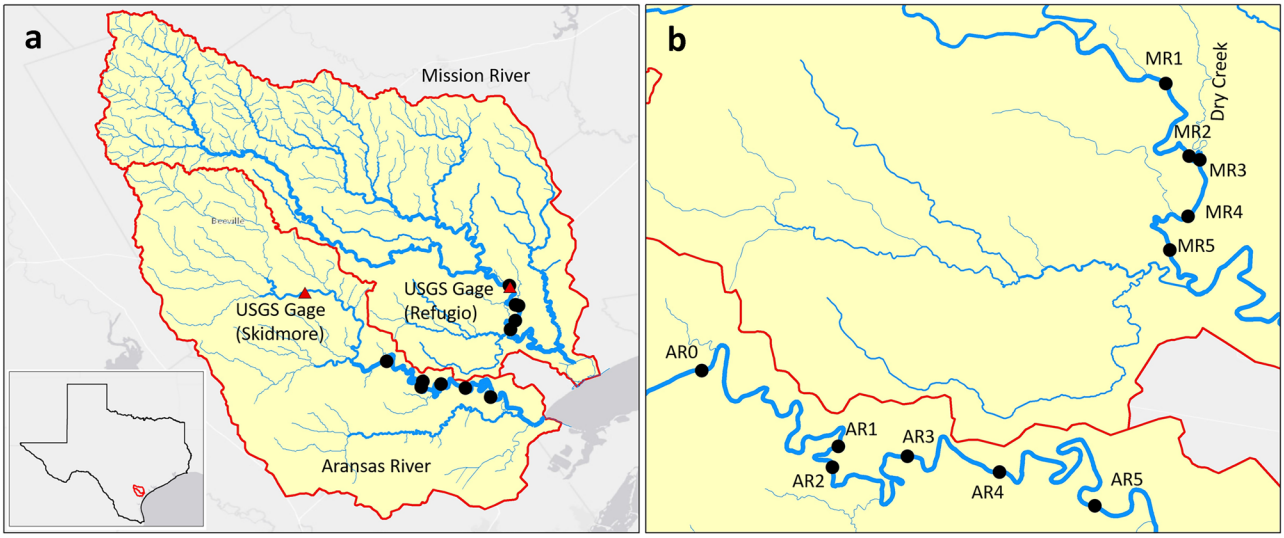

Fig. 1 The Aransas (AR) and Mission (MR) River watersheds (**a**) and sampling stations along the AR and MR (**b**). Red triangles mark USGS water discharge gages at Skidmore (on the AR) and Refugio (on the MR); black circles mark our sampling stations. AR0 and MR1 are above tidal influence. Dry Creek is also labeled in panel **b** because this small tributary delivers wastewater from the town of Refugio to the MR TFZ between MR2 and MR3. The inset map in panel **a** shows the locations of the AR and MR watersheds on the Texas coast

represented the water entering the TFZs from the upstream non-tidal river; the remaining stations were spread along the length of the TFZs at 2–10 km intervals, with sites AR5 and MR5 located most downstream. To ensure that the selected TFZ stations were located within the TFZs throughout the study period, additional flow rate, salinity, and electroconductivity measurements were conducted in a parallel study (Jones 2017; Jones et al. 2020). Occasionally, salinity intrusion occurred at the most downstream site in each river, AR5 and MR5.

Freshwater discharge of the MR and AR is monitored by the United States Geological Survey (USGS) in the non-tidal sections of the rivers at Refugio (gage 08189500) and Skidmore (gage 08189700), respectively (Fig. 1a). These data were verified by the USGS and obtained from the National Water Information System (https://waterdata.usgs.gov/nwis). The MR Refugio gage coincides with MR1, whereas the AR Skidmore gage is ~ 30 km upstream of AR0. The hydrographs at these gages typically feature extended periods of low baseflow (~ 0.2 m^3/s for the AR; 0.3 m^3/s for the MR) interrupted by a few intensive stormflow events each year (peak flow of ~ 17 m^3/s for the AR; ~ 85 m^3/s for the MR; Fig. S1, supplementary material). Water in the lower reaches of the MR and AR is flushed into Copano Bay within hours to a few days during stormflow events, and nutrient concentrations are not significantly different between upstream and downstream locations during these events (Johnson 2009; Mooney and McClelland 2012). During baseflow conditions, however, water residence times within the TFZs are on the order of months (Johnson 2009; Jones et al. 2020). This paper therefore focuses on baseflow conditions. The threshold used in this study to separate baseflow from stormflow is discussed in the section, River discharge calculations for the AR TFZ.

Water Sampling and Analyses

The sampling campaign for this study aimed to capture spatial variations in water chemistry under baseflow conditions during summer and winter over two years. We sampled the MR in summer on June 17, 2015, August 13, 2015, March 3, 2016, June 21, 2016, and July 11, 2016, and in winter on January 15, 2016, January 5, 2017, and February 6, 2017. The March 3, 2016, sampling day was binned into summer as the temperature reached 23 °C, and the conditions were closer to summer. The AR was sampled in summer on June 23, 2015, August 7, 2015, June 14, 2016, July 19, 2016, June 15, 2017, and July 6, 2017, and in winter on January 8, 2016, January 12, 2017, and January 30, 2017. The first three AR field trips (two summers, one winter) sampled stations AR1–AR5. Site AR0 was included in each trip thereafter. Dry Creek, which conveys water from the Refugio WWTP to the MR TFZ (Fig. 1b), was sampled monthly from June 2017 to May 2018.

During each field trip, grab samples for each station were collected in triplicate from the channel center at ~ 10 cm below the surface. Samples for dissolved inorganic N (DIN) and total dissolved N (TDN) analyses were filtered through

0.45-µm polyethersulfone membranes in the field and stored in 150 mL acid-washed HDPE and polycarbonate bottles, respectively. Whole water samples were also collected and stored in 1-L polycarbonate bottles for particulate organic N (PON) and particulate organic carbon (POC) analysis in the laboratory. All samples were transported to the laboratory in coolers, on ice for further processing within 24 h.

In the laboratory, particulate material was concentrated on pre-combusted Whatman GF/F filters (0.7 µm nominal pore size). Water was filtered until throughput slowed to dripping; then filters were dried at 45 °C for a minimum of 24 h and analyzed for PON and POC concentrations and the $\delta^{13}C$ of the particulate material on a Carlo Erba 2500 element analyzer (Elantech, Inc., Lakewood, New Jersey, USA) coupled to a Finnigan MAT 127 Delta^{PLUS} IRMS (Thermo Electron Corporation, Beverly, Massachusetts, USA). DIN was determined as the sum of NO_3^-, NO_2^-, and NH_4^+, which were measured on a QuAAtro auto-analyzer (Seal Analytical Inc., Mequon, Wisconsin, USA) using standard colorimetric methods (EPA 350.1 for NH_4^+ and EPA 353.1 for $NO_3^- + NO_2^-$). TDN was measured with a Shimadzu-TOC-V_{CSH} coupled to a TNM-1 total-N unit (Shimadzu Corporation, Kyoto, Japan) using high-temperature combustion methods, following standard methods (APHA 2012). Dissolved organic N (DON) was calculated by subtracting DIN from TDN. Calculated this way, small errors in DIN propagate into large errors in DON when TDN is dominated by DIN. However, in our dataset, DIN rarely dominated the TDN pool. In > 80% of the samples, DIN was less than half of the TDN, in which cases errors in DON were no greater than errors in DIN. The detection limits for $NO_3^- + NO_2^-$, NH_4^+, and TDN concentrations were 0.36, 0.29, and 0.36 µmol N/L, respectively. For PON mass, the detection limit was 1.5 µmol N. These methods follow those of Mooney and McClelland (2012) and Bruesewitz et al. (2013).

River Discharge Calculations for the AR TFZ

Water discharge into the AR TFZ was estimated by scaling up the daily USGS discharge data from the Skidmore gage (SK) to AR0. The following equation was used to separate WWTP contributions (which do not require scaling) from general watershed runoff contributions (which increase as a function of watershed area):

$$Q_{AR0} = Q_{WWTP} + \left(Q_{SK} - Q_{AR\_WWTP}\right) * A_{AR0}/A_{SK}$$

where Q is flow rate ($m^3\ s^{-1}$) and A is drainage area (km^2). The drainage areas for SK and AR0 are 629 km^2 and 1188 km^2, respectively. These areas were defined in ArcMap 10.6.1 (ESRI, Redlands, CA, USA) using the USGS NHD watershed delineation tool (https://www.usgs.gov/core-science-systems/ngp/national-hydrography/nhd-watershed-tool). Water contributions from WWTPs were estimated as the sum of time-varying inputs from three facilities (Skidmore, Moore Street, and Chasefield) that discharge into the AR upstream of the SK gage. There are no additional WWTP inputs between SK and AR0. WWTP discharge is self-reported by these facilities, and the data were obtained through the United States Environmental Protection Agency Enforcement and Compliance History Online service (https://echo.epa.gov). As mentioned previously, stormflow was excluded in this study. Jones et al. (2019, 2020) defined stormflow conditions in these flashy, semi-arid systems as flows exceeding the 90th percentile of a year of tilt-current meter velocity measurements recorded near the bed of each of the sampling stations during these same sampling years. In accordance with this definition, flow conditions above this threshold were excluded from the analysis. Over the study period, discharge from the three WWTP facilities accounted for ~ 78% of total freshwater discharge at AR0 under baseflow, and ~ 2.7% under stormflow. WWTP discharge did not vary much between baseflow (~ 0.116 m^3/s) and stormflow (~ 0.122 m^3/s).

The tidally influenced baseflow discharge at AR4, near the downstream end of the AR TFZ, was calculated in a parallel study by Jones et al. (2019). In brief, water stage and flow direction data from loggers deployed in the thalweg of the river continuously over the study period (recording at 15-min resolution) were used in combination with periodic discharge measurements using a Sontek Acoustic Doppler Profiler to define a new type of "rating curve" that accounts for tidal effects on stage and discharge, called a "baseflow tidal rating curve." A 3-h moving average was used to remove noise from other forces such as winds before fitting the rating curve. The "baseflow tidal rating curve" was used to estimate the net volumetric discharge across the site's cross-section. The new tidal rating curve method was validated for several river case studies against independently collected and published USGS discharge data, with a mean correlation (R^2) of 0.87 and standard deviation of 0.10 relative to the data from the tidal USGS stations. The tidal rating curve at AR4 was used to estimate instantaneous (15-min intervals) volumetric discharge across the AR4 cross-section (Jones et al. 2019). Baseflow data at AR4 were summed into daily discharge values, to enable daily N flux calculations, and into monthly discharge totals, to check annual water balances. Positive aggregated discharge represented net downstream transport, and negative represented net upstream, during the aggregated time (day or month).

N Flux Calculations for the AR TFZ

Measured N concentrations were combined with estimates of daily discharge at AR0 and AR4 to quantify daily N fluxes into and out of the AR TFZ during winter (December, January, and February) and summer (June, July, and August)

from 2015 to 2017. Specifically, the median value of all measured N concentrations in each season was used to represent the N concentration in every day of that season and was multiplied by the daily water discharge. The resulting daily N fluxes were then summed for each season and compared between AR0 and AR4.

Data Visualization and Analyses

The concentrations of N in different forms, at each measurement location and in each season, were summarized in Tukey-style box-whisker plots generated with the R package ggplot2 (Wickham 2016). Spatial patterns were visualized by comparing boxplots among sites within the same river. Median N concentrations, and the ratio between total organic N (TON, the sum of PON and DON) and DIN, were compared statistically between the input water and the TFZ water, and between the AR and MR waters, using Kruskal–Wallis tests. Differences between monthly mean discharges at AR0 and AR4 were tested with paired t-tests. The Kruskal–Wallis tests and *t*-tests were performed at a 95% confidence level using IBM SPSS Statistics for Windows Version 25.0 (IBM Crop., Armonk, NY, USA).

Results

Spatial and Seasonal Patterns

Quantities of N within the AR and MR TFZs varied substantially over space and time. DIN showed the largest variations among sampling locations and between seasons (Figs. 2 and 3). Concentrations of DIN were generally higher in winter than summer and exhibited gradients associated with the locations of major DIN inputs. DIN concentrations decreased from upstream to downstream in the AR (Fig. 2a, e), whereas DIN concentrations peaked in the middle of the MR TFZ immediately downstream of the Dry Creek input of WWTP water (Fig. 3a, e). Patterns for TN largely paralleled those described for DIN. These spatial patterns for DIN and TN were more pronounced during winter than summer, but DIN was correlated with TN during both seasons (Spearman coefficients of 0.93 and 0.67 in summer and 0.73 and 0.34 in winter, for the AR and MR, respectively). In contrast with DIN, concentrations of organic N (DON and PON) were more uniform among sampling locations and between seasons, although there was a notable trend of increasing PON downstream through the AR TFZ (Fig. 2g), and increasing DON in the MR TFZ, in summer (Fig. 3f).

POC/PON ratios ranged from 5 to 10 and generally remained stable along the AR TFZ (Fig. 4a, b), whereas the ratios were more variable but generally increased along the MR TFZ (Fig. 4e, f). The $\delta^{13}C$ values of the particulate material ranged from −22 to −35‰ across both rivers but did not show a clear upstream–downstream trend in either of the rivers (Fig. 4c, d, g, h). The median $\delta^{13}C$ value of all TFZ stations of both rivers combined was −32‰ (Fig. 4c, d, g, h).

Comparison of N in TFZ and Non-tidal River Waters

Amounts and forms of N differed substantially between the TFZs and their upstream influent waters (Table 1). The median TON/DIN ratio in the AR TFZ was ~ 7 times higher than in its input water ($p = 0.07$), and for the MR TFZ, the ratio was ~ 2.7 times higher ($p = 0.02$). The higher median TON/DIN in the AR TFZ was driven both by the lower median DIN ($p = 0.08$) and higher median PON ($p < 0.001$) in the TFZ water compared to its upstream river input. In contrast, in the MR TFZ, the higher median TON/DIN ratio was driven only by higher median DIN, which was 3.3 times higher in the input river water than in the TFZ water ($p = 0.01$). There was no substantial difference in DON between the TFZ and its upstream input waters in either river. Median TN was 48% lower in the TFZ than the input for the AR ($p = 0.2$), and 31% lower in the TFZ than the input for the MR ($p = 0.15$). These differences in median TN between TFZ and input water were relatively weak statistically, but consistent in sign and magnitude for both rivers. Overall, median TN concentrations were higher in the AR than the MR. However, the differences were more statistically discernable when comparing the TFZs ($p = 0.01$) than when comparing the inputs ($p = 0.52$).

Water and N Fluxes in the AR

In addition to the seasonal changes in N concentrations in the rivers and their TFZs, temporal changes in river flows must be accounted for to better understand N export to the TFZ-influenced coast. Average monthly water influent to the AR TFZ from upstream was relatively constant under baseflow conditions, while average monthly TFZ outflow varied strongly over seasonal timeframes (Fig. 5). AR TFZ outflow greatly exceeded inflow in January and February (coincident with our winter sampling period). The opposite was true during April, May, September, October, and November. In fact, negative values at AR4 during these months indicated net upstream flow within the lower reaches of the TFZ due to the seasonal secular tides (Jones et al. 2020). During June–August (our summer sampling period), inflows and outflows were more balanced. Inflow to the AR TFZ was greater than outflow during July, and less than outflow during August, but on average, for June–August, they were not markedly different. Overall, the variations in flow rate and direction

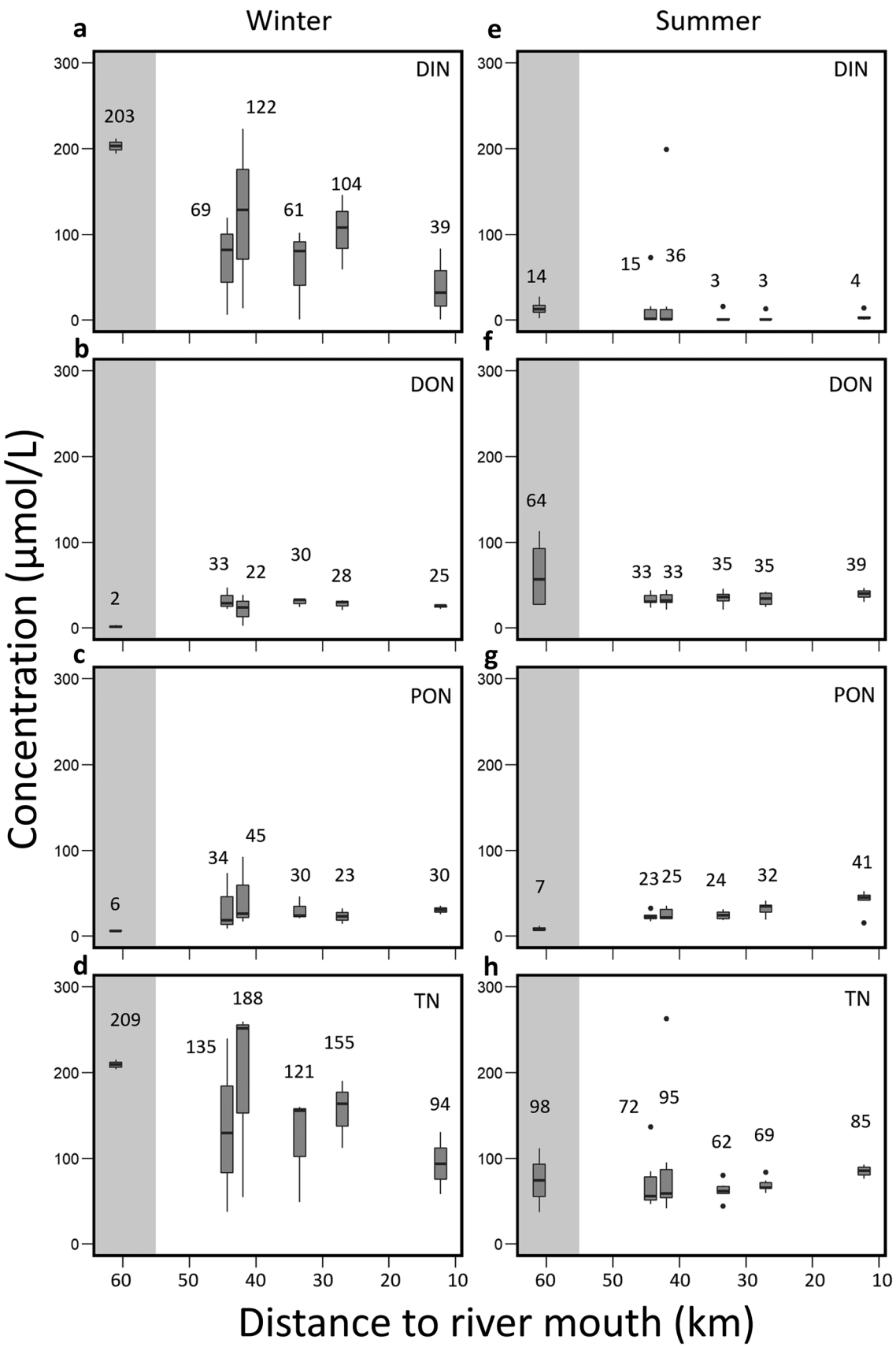
Winter
Summer
a
b
c
d
e
f
g
h
DIN
DON
PON
TN
Concentration (µmol/L)
Distance to river mouth (km)
0
100
200
300
60
50
40
30
20
10
203
122
69
61
104
39
14
15
36
3
3
4
2
33
22
30
28
25
64
33
33
35
35
39
6
34
45
30
23
30
7
23
25
24
32
41
209
188
135
121
155
94
98
72
95
62
69
85

◂**Fig. 2** Boxplots of N concentrations in the AR during winter (**a**, **b**, **c**, **d**) and summer (**e**, **f**, **g**, **h**). Shaded areas highlight non-tidal inputs at AR0. All other boxes are within the AR TFZ. Box size indicates the interquartile range (IQR); whiskers represent 1.5 × IQR; the center band presents the median; the number above each box is the mean. Values beyond 1.5 × IQR are treated as outliers and are shown as points

at AR4 were strongly tied to variations in sea levels in Copano Bay (Fig. 5). Secular tidal variations facilitated net accumulation of fresh water within the TFZ during some times of the year and net losses of fresh water during other times, but inflow and outflow were balanced on an annual basis (i.e., monthly inflows were not significantly different than monthly outflows when averaged annually; $p = 0.08$, t-test).

Patterns in N input to the AR TFZ at AR0 and net downstream export at AR4 were tightly coupled to the freshwater flow (Table 2). During summer, when water inflows and outflows were essentially balanced, TN input and export were quite similar. During winter, when water outflows were much greater than TFZ inflows, TN export far exceeded TN input.

Discussion

Because of their locations at the downstream ends of river networks, TFZs may play a particularly important role in modifying N fluxes from watersheds to estuaries. Our understanding of relationships between N inputs and estuarine responses has not, to date, adequately accounted for production/removal and transformations within TFZs. Our results suggest that TFZs facilitate the conversion of inorganic N to organic forms (especially PON) during their extended water residence times during baseflow conditions (Jones et al. 2017). Furthermore, our seasonal flux comparisons suggest that TFZ inflow/outflow dynamics can substantially alter the timing of watershed-derived N export to estuaries. In the AR case, seasonal variations in N concentrations and secular tidal effects together resulted in much larger N export than input during winter. This contrasted with summer, where input and export were approximately balanced. More data are needed to develop a complete annual N budget for the AR TFZ, but patterns in freshwater inflow versus outflow point to different periods throughout the year when net N accumulation and release are likely occurring.

Water Column N Concentrations

Spatial patterns in water column N within the AR and MR systems suggest that TFZs support net conversion of inorganic N inputs to organic forms. This is exemplified by the overall shift toward lower DIN concentrations and higher TON/DIN ratios from non-tidal to TFZ waters (Table 1). Differences in spatial patterns between the two TFZs are related to where major wastewater inputs are located within each watershed. Lateral inputs to MR from Dry Creek (Fig. 1b) are responsible for peaks in DIN concentrations just downstream of that location during both seasons (Fig. 3a, e), and for the associated peak in PON during winter (Fig. 3c). Peak DIN concentrations (both winter and summer, Fig. 2a, e) and PON concentrations (winter, Fig. 2c) near the upper extent of the AR TFZ are consistent with major wastewater inputs coming from upstream in that watershed. The stronger spatial patterns in winter compared to summer are likely due to the higher N levels in the influent water during winter. While we did not directly measure N inputs from WWTPs in this study, their importance is also suggested by considering how much of the freshwater inflow comes from WWTPs under baseflow conditions. WWTP discharge made up ~ 78% of freshwater discharge at AR0 and ~ 30% of freshwater discharge at MR0 during baseflow (the current study, and Mooney and McClelland 2012).

The increase in PON concentrations downstream of N inputs is most likely caused by phytoplankton production. The average POC/PON ratio (7.1 and 8.0 for the AR and MR, respectively, Fig. 4) fell within the range reported for riverine phytoplankton (They et al. 2017), and the range of $\delta^{13}C$ values of particulate organic matter (−22 to −35‰, median −32‰, Fig. 4) also covered the expected range for freshwater phytoplankton (Cloern et al. 2002). Chlorophyll data from the AR further support the interpretation that the changing N forms within the TFZs relate to phytoplankton production. Although we did not measure chlorophyll, concentrations of chlorophyll-a (chl a) are monitored by the Texas Commission on Environmental Quality at three sampling stations along the AR (station IDs: 12952, 12948, and 12947; data available through the Texas Clean River Program; https://www.tceq.texas.gov/waterquality/clean-rivers). Station 12952 coincides with the USGS Skidmore gage on the AR, 12948 is located between AR1 and AR2 near the upper end of the TFZ, and 12947 is between AR4 and AR5, more downstream in the TFZ. The long-term records from these stations (1982–2017) demonstrate that chl a increases downstream, with average concentrations increasing from 3.2 to 12.4 to 15.7 µg/L moving from upstream to downstream among these three AR stations. This multi-year record of chl a increasing downstream further supports the idea that the increase of PON with distance downstream in the TFZ is caused by phytoplankton production.

Prolonged water residence times in the TFZs under baseflow conditions likely facilitate the conversion of inorganic to organic N (particularly by supporting persistent phytoplankton blooms). In a study focusing on fecal coliform

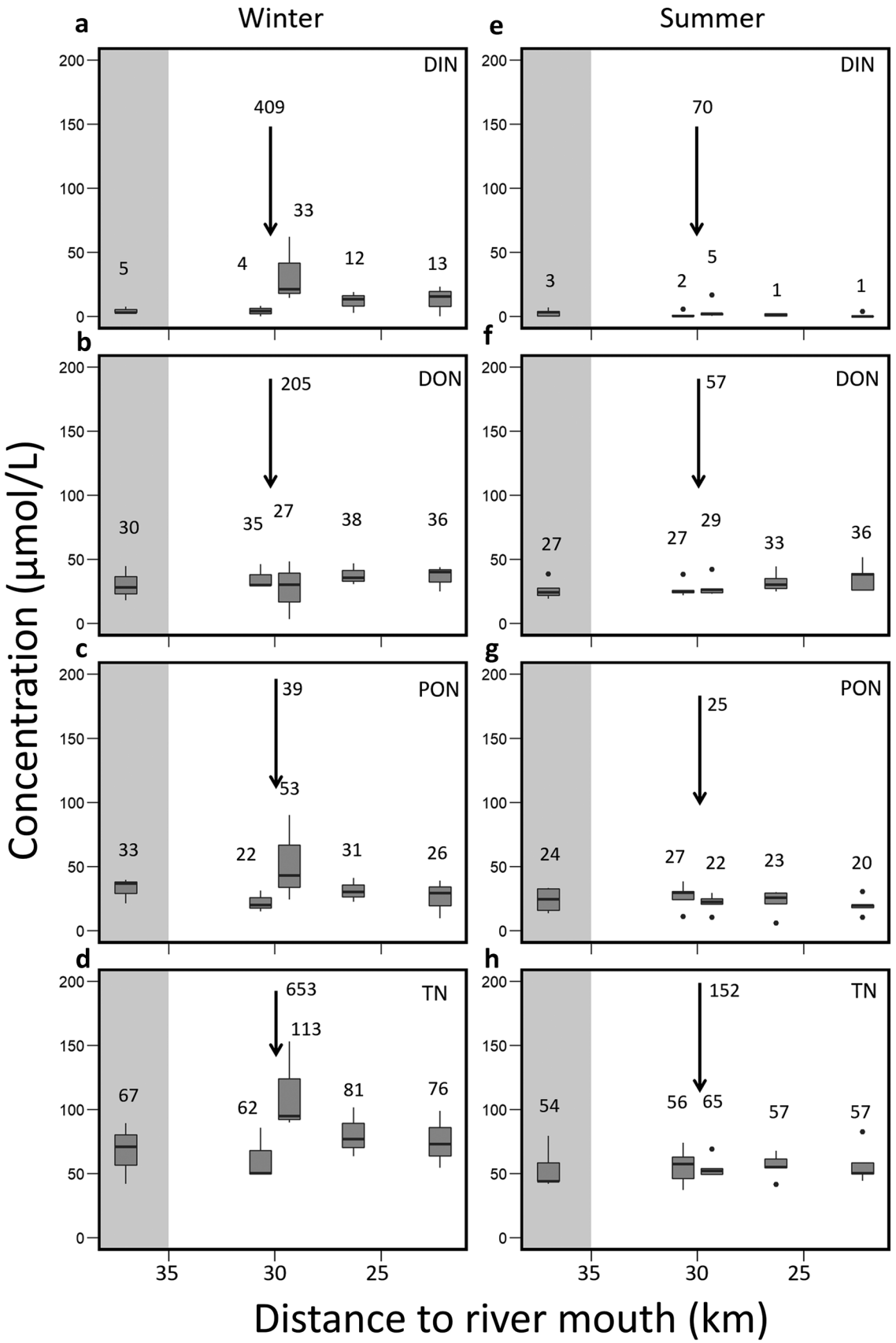
a
Winter
e
Summer
DIN
b
DON
f
c
PON
g
d
TN
h
Concentration (µmol/L)
Distance to river mouth (km)
35
30
25
0
50
100
150
200
5
409
33
4
12
13
3
70
5
2
1
1
30
205
27
35
38
36
27
57
29
27
33
36
33
39
53
22
31
26
24
25
27
22
23
20
67
653
113
62
81
76
54
152
56
65
57
57

◂**Fig. 3** Boxplots of N concentrations in the MR during winter (**a**, **b**, **c**, **d**) and summer (**e**, **f**, **g**, **h**). Shaded areas highlight non-tidal inputs at MR1. All other boxes are within the MR TFZ. Box size indicates the interquartile range (IQR); whiskers represent 1.5 × IQR; the center band presents the median; the number above each box is the mean. Values beyond 1.5 × IQR are treated as outliers and are shown as points. Arrows and associated values (means) mark WWTP inputs via Dry Creek to the MR TFZ

contamination, Johnson (2009) estimated that water residence times in the AR and MR TFZs were 6–9 months. More recent work by Jones et al. (2017) suggests that residence times could be substantially longer under extended drought conditions. In contrast, residence times in the upstream non-tidal AR and MR are typically a few days (Bruesewitz et al. 2017).

Another possible source of PON in the AR and MR TFZs is terrestrial detritus input, but previous work has shown that contributions from the surrounding watersheds to suspended PON in the upstream, non-tidal sections of these rivers are low during baseflow conditions (Mooney and McClelland 2012). Bank erosion within the MR and AR TFZs has not been quantified but is an unlikely source of terrestrial PON input to these TFZs under baseflow conditions; no evidence of active bank erosion was observed during field trips for this study.

N Input/Export Dynamics in the AR System

Wet/dry climate patterns are recognized as important controls on phytoplankton dynamics and ecosystem metabolism in south Texas estuaries (Bruesewitz et al. 2013; Reyna et al. 2017), but the effects of TFZs on the timing of freshwater and material export to estuaries have not been widely explored. Our seasonal flux estimates demonstrate how tidal influences and biogeochemical processing affect freshwater and N export from the TFZ during different times of a year. Both seasonal and tidal factors that alter TFZ inflow/outflow dynamics can substantially alter not only the quantity and chemical form of watershed-derived N exported to estuaries but also the timing of such exports.

Evapotranspiration effects and lateral groundwater inputs are considered relatively minor compared to surface water flows in the AR system. Evaporative losses were estimated to average ~ 0.03 m^3/s based on monthly evaporation data published by the Texas Water Board (https://waterdatafortexas.org/lake-evaporation-rainfall) and the surface area of the AR TFZ (804,571 m^2). Transpiration was assumed to be small because the AR TFZ has little fringing vegetation. Groundwater flows in this area are poorly understood (Evans et al. 2012), but preliminary measurements from artesian wells by the Mission Aransas National Estuary Research Reserve show low discharge rates (~ 0.005 m^3/s, unpublished data). These rates are 1–2 orders of magnitude smaller than freshwater inflows via the AR to the TFZ (Fig. 5).

Ruling out such distributed withdrawals or inputs, the water balance for the AR TFZ suggests that the timing of freshwater accumulation and release was strongly influenced by secular tidal variations that greatly affected the mean sea level of the downstream receiving waters of Copano Bay (Fig. 5). These tidal variations had a determinative effect on the N fluxes despite different N concentration patterns in summer and winter (Fig. 2). Water and N export from the TFZ to the estuary were higher than input to the TFZ by its upstream river inflow during the winter season (December–February, Table 2). The semiannual low tide in the Gulf of Mexico probably drew mean sea level down in Copano Bay during winter, which contributed to the observed high TFZ export (Fig. 5). Other forces, such as wind-driven movement in Copano Bay and Ekman transport along the Gulf coast, could also have affected TFZ dynamics, which was convolved into the tidal variations captured by the loggers, although local wind effects on the TFZ water column were filtered as noise in the estimation of TFZ discharges (Jones et al. 2019).

There was also evidence for N removal within the AR TFZ during winter after normalizing for water discharge: water outflow was ~ 5 times greater than water inflow in the winter, whereas TN export was only ~ 4 times greater than TN input (Table 2), suggesting ~ 20% of TN removal. This is comparable to TN removal reported for other TFZs, such as James River TFZ (32%, Bukaveckas and Isenberg 2013) and the Hudson River TFZ (15%, Lampman et al. 1999). Although this ~ 20% loss of N relative to the water balance during winter is not well constrained, the winter TN flux results suggest that net N removal occurred within the AR TFZ during at least some times of year. This contrasted with summer (June–August), when inputs and exports were approximately balanced (Table 2). In any case, the flux estimates presented in Table 2 are consistent with our concentration results, showing strong evidence for conversion of inorganic N input to organic matter export within the TFZs during baseflow conditions.

In all remaining months (April, May, September, October, and November), the negative discharge data at AR4 points to net upstream flow in the lower TFZ when averaged over monthly time intervals (Fig. 5). During these months, net accumulation of water likely occurred in the AR TFZ despite daily tidal cycles, due to secular tidal variations (Jones et al. 2020). Reversed net transport of water (i.e., upstream transport) in the lower portions of TFZs over monthly and longer periods has been similarly documented in other studies (Chen et al. 2005; Burchard et al. 2018; Jones et al. 2019, 2020). Reduced or reversed net discharge in the lower reaches of TFZs can have implications for solute processing and export to downstream systems. For example, during those spring and fall months with net negative discharges, the AR TFZ likely retained N, regardless of the N

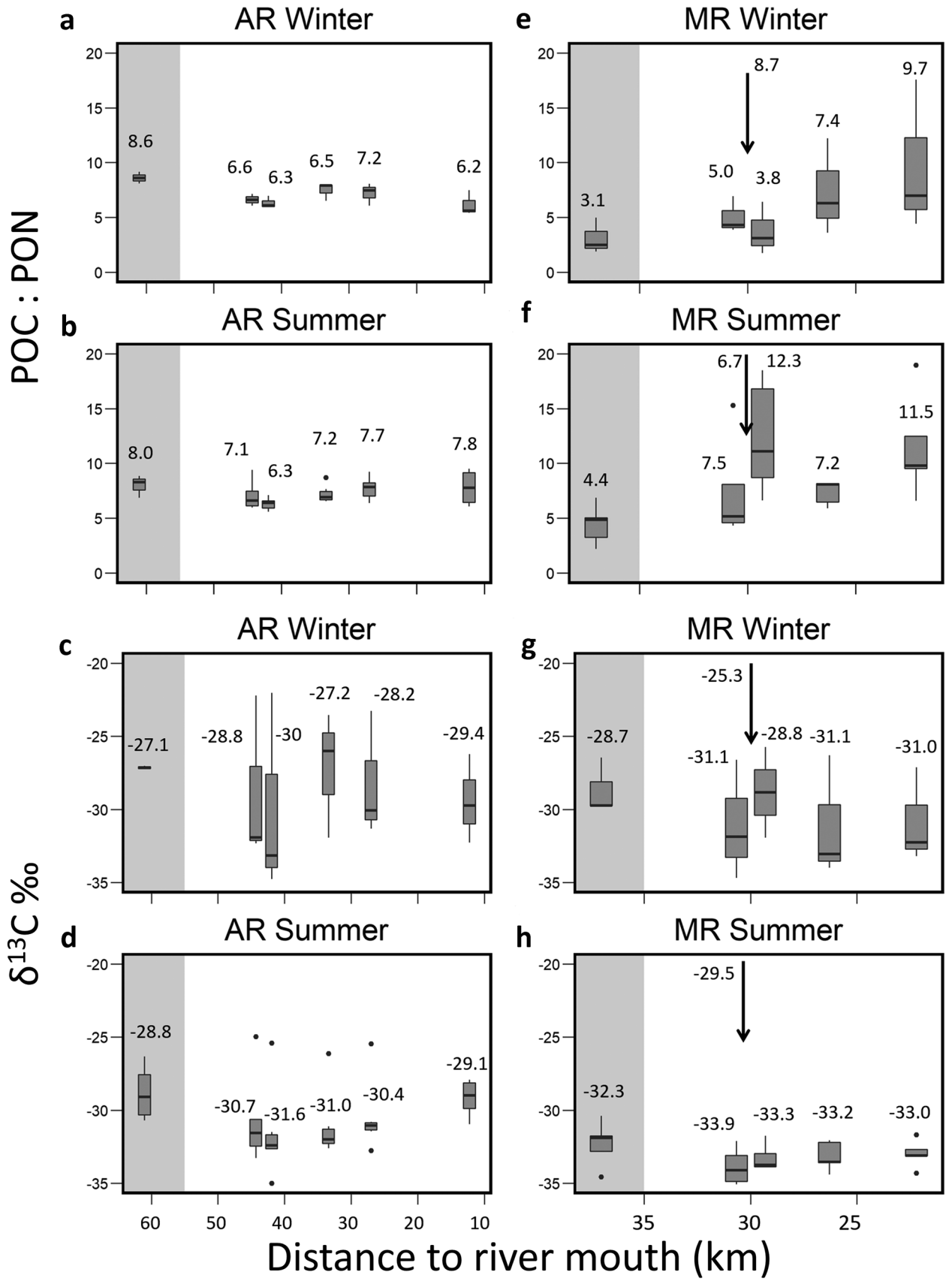
a
AR Winter
8.6
6.6
6.3
6.5
7.2
6.2
b
AR Summer
8.0
7.1
6.3
7.2
7.7
7.8
e
MR Winter
3.1
5.0
8.7
3.8
7.4
9.7
f
MR Summer
4.4
7.5
6.7
12.3
7.2
11.5
c
AR Winter
-27.1
-28.8
-30
-27.2
-28.2
-29.4
d
AR Summer
-28.8
-30.7
-31.6
-31.0
-30.4
-29.1
g
MR Winter
-28.7
-31.1
-25.3
-28.8
-31.1
-31.0
h
MR Summer
-32.3
-33.9
-29.5
-33.3
-33.2
-33.0
POC : PON
δ13C ‰
Distance to river mouth (km)

◂**Fig. 4** Boxplots of POC/PON and $\delta^{13}C$ values of POC in the AR and MR during winter and summer. Shaded areas highlight non-tidal stations (AR0 and MR1). All other boxes are within the TFZ. Box size indicates the interquartile range (IQR); whiskers represent 1.5×IQR; the center band presents the median; the number above each box is the mean. Values beyond 1.5×IQR are treated as outliers and are shown as points. Arrows and associated values (means) mark WWTP inputs via Dry Creek to the MR TFZ

concentration and form. Since we did not measure N concentrations for every month of the year, more data are needed to build an annual N budget for this system.

While pulses of storm flow account for a large proportion of the fresh water and nutrients delivered to Copano Bay each year (Mooney and McClelland 2012; Bruesewitz et al. 2013; Reyna et al. 2017), the data presented herein demonstrate how temporal variations in retention/release associated with secular tidal patterns also have a strong influence on the timing of inputs to the bay. TFZ dynamics may play a particularly important role in regulating wastewater N export from watersheds to estuaries, as discharges from WWTPs to rivers are an important source of freshwater during dry periods.

Table 1 Median concentrations (µmol/L) of different forms of N in the AR and MR TFZs and non-tidal input waters. Differences in median values were tested between input and TFZ waters for each river, and between the AR and MR, using Kruskal–Wallis tests. The reported statistics of the Kruskal–Wallis test on the medians include the chi^2 and the associated *p*-value

	River	Station/Stats	DIN	DON	PON	TN	TON/DIN
Median	AR	Input	20.5	27.7	6.71	146	4.42
		TFZ	2.52	31.0	25.7	76.3	32.6
	MR	Input	7.31	33.6	26.9	84.3	9.90
		TFZ	2.19	30.2	24.7	58.0	26.4
Input vs. TFZ	AR	Chi^2	2.98	0.28	13.00	1.63	3.22
		p	0.08	0.60	0.00	0.20	0.07
	MR	Chi^2	6.05	0.21	0.74	2.12	5.47
		p	0.01	0.65	0.39	0.15	0.02
AR vs. MR	Input	Chi^2	0.55	0.083	10.5	0.42	1.23
		p	0.46	0.77	0.00	0.52	0.27
	TFZ	Chi^2	2.6	0.069	1.27	6.57	2.25
		p	0.11	0.79	0.26	0.01	0.13

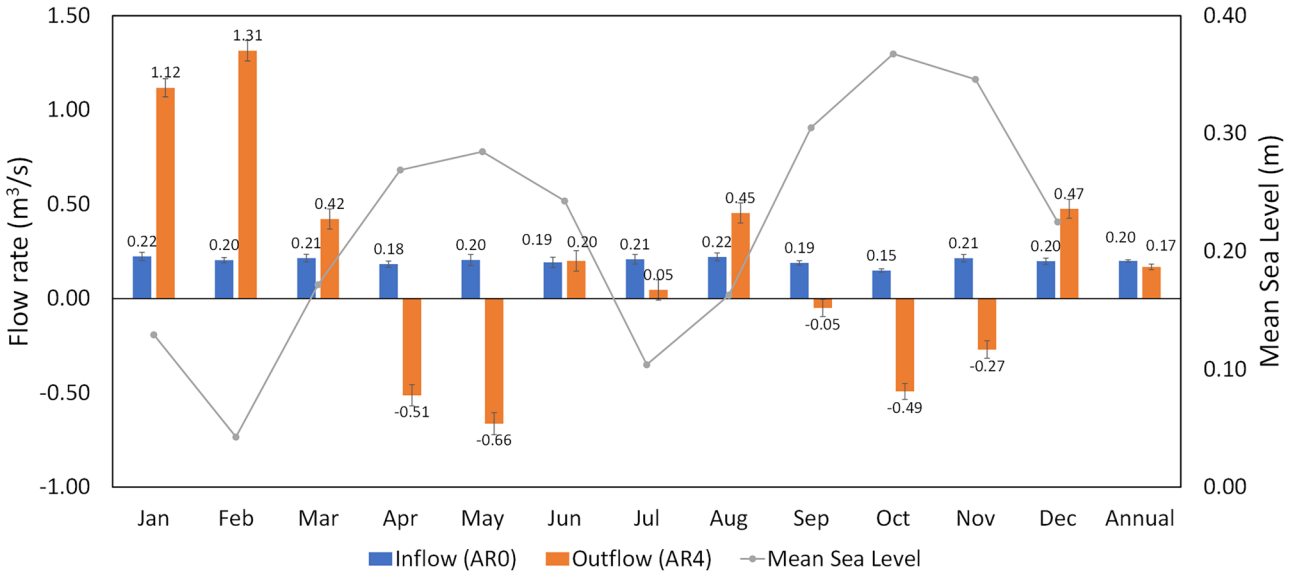

Fig. 5 Mean monthly flow rates for 2015–2017 at AR0 (blue columns) and AR4 (orange columns) from Jones et al. (2019) and monthly mean sea level (grey lines) in Copano Bay from the National Oceanic and Atmospheric Administration tide gauge 8774770 (https://tidesandcurrents.noaa.gov). Flows at AR0 represent upstream, non-tidal river inputs to the AR TFZ, while flows at AR4 represent TFZ export (positive) or temporary freshwater accumulation in the TFZ (negative). Bar heights and values above the bars are mean monthly flow rates (m^3/s), and error bars represent the standard error of the means

Table 2 Daily average water flow ± mean standard error (m^3/s), and estimated daily average N flux ± mean standard error (kg/d), at AR0 (non-tidal TFZ influent) and AR4 (downstream TFZ effluent) across summers (June, July, and August) and winters (December, January, and February) of 2015–2017

		Flow	DIN	DON	PON	TN
Summer	AR0	0.20 ± 0.01	2.5 ± 0.13	14 ± 0 .71	1.9 ± 0.10	19 ± 1.0
	AR4	0.23 ± 0.03	0.2 ± 0.02	9.7 ± 1.1	9.8 ± 1.1	18 ± 2.1
Winter	AR0	0.19 ± 0.01	47 ± 2.1	0.4 ± 0.02	1.4 ± 0.06	48 ± 2.2
	AR4	0.97 ± 0.03	126 ± 3.2	35 ± 0.89	27 ± 0.68	192 ± 4.8

Summary and Conclusions

To better understand the role of TFZs in modifying N fluxes at the river/estuary interface, we compared concentrations and forms of N in the MR and AR TFZs to concentrations and forms of N in the upstream non-tidal river waters during different seasons (winter versus summer) over a two-year period. We also compared N fluxes in winter and summer in the AR TFZ to understand how tidal dynamics and biogeochemistry together affect N export to the estuary. Spatial patterns of N concentrations and forms varied between the AR and MR, reflecting different amounts and locations of WWTP inputs to these two systems. Patterns within both systems demonstrated that the TFZs promote conversion of DIN into PON (mainly phytoplankton). Meanwhile, secular tidal patterns can modulate the timing of baseflow N export at monthly to annual scales. In particular, we found that N export far exceeded N input for the AR TFZ during winter (although discharge-normalized N flux estimates suggested that ~ 20% of TN inputs were removed within the AR TFZ). While more data are needed to build an annual N budget, our results show that TFZ can change the timing and form of N export immediately upstream of estuaries. This paper adds to the very limited number of publications on N biogeochemistry in TFZs, and highlights the role of secular tidal dynamics in modulating N export, a previously unexplored aspect for TFZ biogeochemistry.

Supplementary Information The online version contains supplementary material available at https://doi.org/10.1007/s12237-022-01112-7.

Acknowledgements We thank the REUisME program (NSF #1358890) led by Dr. Deana Erdner and the University of Texas at Austin Semester-by-the-Sea program. Both programs supported undergraduate researchers Grayson Barker, Kylie Holt, Spyder Julian, Tricia Light, Sierra Melton, and Ana Salamanca, who assisted with this project in the field and lab. We also thank Dr. Ryan Hladyniuk and Patricia Garlough for analyzing the particulate organic nutrient samples. This work would not have been possible without their help.

Author Contribution Amber Hardison, James McClelland, and Kevan Moffett conceived and designed the research, Hengchen Wei and Xin Xu collected the biogeochemical data, Allan Jones measured and modeled the discharge data, all authors contributed to the data analysis, Hengchen Wei wrote the original draft, and all authors contributed to the revision of the manuscript.

Funding This study is supported by the National Science Foundation (#1417433).

Data Availability Available online.

Declarations

Conflict of Interest The authors declare no competing interests.

References

Amphlett, M.B., and T.E. Brabben. 1990. Measuring freshwater flows in large tidal rivers. *Water management of the Amazon Basin Manaus* 5–9.

APHA. 2012. *Standard methods for the examination of water and wastewater*, 22nd ed. American Water Works Association, Water Environment Federation: American Public Health Association.

Arndt, S., G.G. Lacroix, N. Gypens, P. Regnier, and C. Lancelot. 2011. Nutrient dynamics and phytoplankton development along an estuary-coastal zone continuum: A model study. *Journal of Marine Systems* 84. Elsevier B.V.: 49–66. https://doi.org/10.1016/j.jmarsys.2010.08.005.

Boesch, D.F. 2002. Challenges and opportunities for science in reducing nutrient over-enrichment of coastal ecosystems. *Estuaries* 25. Springer: 886–900. https://doi.org/10.1007/BF02804914.

Bruesewitz, D.A., W.S. Gardner, R.F. Mooney, L. Pollard, and E.J. Buskey. 2013. Estuarine ecosystem function response to flood and drought in a shallow, semiarid estuary: Nitrogen cycling and ecosystem metabolism. *Limnology and Oceanography* 58: 2293–2309. https://doi.org/10.4319/10.2013.58.6.2293.

Bruesewitz, D.A., T.J. Hoellein, R.F. Mooney, W.S. Gardner, and E.J. Buskey. 2017. Wastewater influences nitrogen dynamics in a coastal catchment during a prolonged drought. *Limnology and Oceanography* 62. Wiley Online Library: S239–S257. https://doi.org/10.1002/lno.10576.

Bukaveckas, P.A., and W.N. Isenberg. 2013. Loading, transformation, and retention of nitrogen and phosphorus in the tidal freshwater James River (Virginia). *Estuaries and Coasts* 36: 1219–1236. https://doi.org/10.1007/s12237-013-9644-x.

Burchard, H., H.M. Schuttelaars, and D.K. Ralston. 2018. Sediment trapping in estuaries. *Annual Review of Marine Science* 10: 371–395. https://doi.org/10.1146/annurev-marine-010816-060535.

Chen, M.S., S. Wartel, B. van Eck, and D. van Maldegem. 2005. Suspended matter in the Scheldt estuary. *Hydrobiologia* 540: 79–104. https://doi.org/10.1007/s10750-004-7122-y.

Cloern, J.E., E.A. Canuel, and D. Harris. 2002. Stable carbon and nitrogen isotope composition of aquatic and terrestrial plants of the San Francisco Bay estuarine system. *Limnology and Oceanography* 47: 713–729. https://doi.org/10.4319/lo.2002.47.3.0713.

Cloern, J.E. 2001. Our evolving conceptual model of the coastal eutrophication problem. *Marine Ecology Progress Series* 210: 223–253. https://doi.org/10.3354/meps210223.

Conner, W.H., T.W. Doyle, and K.W. Krauss. 2007. *Ecology of tidal freshwater forested wetlands of the southeastern United States*. Dordrecht: Springer, Netherlands. https://doi.org/10.1007/978-1-4020-5095-4.

Ensign, S.H., M.W. Doyle, M.F. Piehler, N. Carolina, and C. Hill. 2013. The effect of tide on the hydrology and morphology of a freshwater river. *Earth Surface Processes and Landforms* 38: 655–660. https://doi.org/10.1002/esp.3392.

Ensign, S.H., and G.B. Noe. 2018. Tidal extension and sea-level rise: Recommendations for a research agenda. *Frontiers in Ecology and the Environment* 16: 37–43. https://doi.org/10.1002/fee.1745.

Evans, A., K. Madden, and S. Palmer. 2012. The ecology and sociology of the Mission-Aransas estuary: An estuarine and watershed profile.

Findlay, S., M. Pace, and D. Lints. 1991. Variability and transport of suspended sediment, particulate and dissolved organic carbon in the tidal freshwater Hudson River. *Biogeochemistry* 12: 149–169. https://doi.org/10.1007/BF00002605.

Guo, L., M. van der Wegen, D.A. Jay, P. Matte, Z.B. Wang, D. Roelvink, and Q. He. 2015. River-tide dynamics: Exploration of nonstationary and nonlinear tidal behavior in the Yangtze River estuary. *Journal of Geophysical Research: Oceans* 120: 3499–3521. https://doi.org/10.1002/2014JC010491.

Halpern, B.S., S. Walbridge, K.A. Selkoe, C.V. Kappel, F. Micheli, C. D'Agrosa, J.F. Bruno, et al. 2008. A global map of human impact on marine ecosystems. *Science* 319: 948–952. https://doi.org/10.1126/science.1149345.

Hellings, L., F. Dehairs, M. Tackx, E. Keppens, and W. Baeyens. 1999. Origin and fate of organic carbon in the freshwater part of the Scheldt Estuary as traced by stable carbon isotope composition. *Biogeochemistry* 47: 167–186. https://doi.org/10.1007/BF00994921.

Hoitink, A.J.F., and D.A. Jay. 2016. Tidal river dynamics: Implications for deltas. *Reviews of Geophysics* 54: 240–272. https://doi.org/10.1002/2015RG000507.

Johnson, S.L. 2009. A general method for modeling coastal water pollutant loadings. The University of Texas at Austin.

Jones, A.E. 2017. Where the river meets the sea : An initial investigation into the Riverine Tidal Freshwater Zone. The University of Texas at Austin.

Jones, A.E., A.K. Hardison, B.R. Hodges, J.W. McClelland, and K.B. Moffett. 2019. An expanded rating curve model to estimate river discharge during tidal influences across the progressive-mixed-standing wave systems. *Edited by Weili Duan. PLOS ONE* 14: e0225758. https://doi.org/10.1371/journal.pone.0225758.

Jones, A.E., A.K. Hardison, B.R. Hodges, J.W. McClelland, and K.B. Moffett. 2020. Defining a riverine tidal freshwater zone and its spatiotemporal dynamics. *Water Resources Research*. https://doi.org/10.1029/2019WR026619.

Jones, A.E., B.R. Hodges, J.W. McClelland, A.K. Hardison, and K.B. Moffett. 2017. Residence-time-based classification of surface water systems. *Water Resources Research* 53: 5567–5584. https://doi.org/10.1002/2016WR019928.

Jones, R.C., D.P. Kelso, and E. Schaeffer. 2008. Spatial and seasonal patterns in water quality in an embayment-mainstem reach of the tidal freshwater Potomac River, USA: A multiyear study. *Environmental Monitoring and Assessment* 147: 351–375. https://doi.org/10.1007/s10661-007-0126-0.

Lampman, G.G., N.F. Caraco, and J.J. Cole. 1999. Spatial and temporal patterns of nutrient concentration and export in the tidal Hudson River. *Estuaries* 22: 285. https://doi.org/10.2307/1352984.

Lebo, M.E., and J.H. Sharp. 1993. Distribution of phosphorus along the Delaware, an urbanized coastal plain estuary. *Estuaries* 16: 290. https://doi.org/10.2307/1352502.

Lotze, H.K. 2006. Depletion, degradation, and recovery potential of estuaries and coastal seas. *Science* 312: 1806–1809. https://doi.org/10.1126/science.1128035.

Lovley, D.R., and E.J.P. Phillips. 1986. Availability of ferric iron for microbial reduction in bottom sediments of the freshwater tidal Potomac River. *Applied and Environmental Microbiology* 52: 751–757. https://doi.org/10.1128/AEM.52.4.751-757.1986.

Megonigal, J.P., and S.C. Neubauer. 2019. Biogeochemistry of tidal freshwater wetlands. In *Coastal Wetlands*, ed. G. M. E. Perillo, E. Wolanski, D. Cahoon, and C. Hopkinson, 2nd ed., 641–683. Elsevier. https://doi.org/10.1016/B978-0-444-63893-9.00019-8.

Minaudo, C., F. Moatar, A. Coynel, H. Etcheber, N. Gassama, and F. Curie. 2016. Using recent high-frequency surveys to reconstitute 35 years of organic carbon variations in a eutrophic lowland river. *Environmental Monitoring and Assessment* 188: 41. https://doi.org/10.1007/s10661-015-5054-9.

Mooney, R.F., and J.W. McClelland. 2012. Watershed export events and ecosystem responses in the Mission-Aransas National Estuarine Research Reserve, South Texas. *Estuaries and Coasts* 35: 1468–1485. https://doi.org/10.1007/s12237-012-9537-4.

Nowacki, D.J., A.S. Ogston, C.A. Nittrouer, A.T. Fricke, N.E. Asp, and P.W.M. Souza Filho. 2019. Seasonal, tidal, and geomorphic controls on sediment export to Amazon River tidal floodplains. *Earth Surface Processes and Landforms*: esp. 4616. https://doi.org/10.1002/esp.4616.

Peterson, B.J. 2001. Control of nitrogen export from watersheds by headwater streams. *Science* 292: 86–90. https://doi.org/10.1126/science.1056874.

Reyna, N.E., A.K. Hardison, and Z. Liu. 2017. Influence of major storm events on the quantity and composition of particulate organic matter and the phytoplankton community in a subtropical estuary, Texas. *Frontiers in Marine Science* 4: 43. https://doi.org/10.3389/fmars.2017.00043.

Romero, E., R. le Gendre, J. Garnier, G. Billen, C. Fisson, M. Silvestre, and P. Riou. 2016. Long-term water quality in the lower Seine: Lessons learned over 4 decades of monitoring. *Environmental Science & Policy* 58: 141–154. https://doi.org/10.1016/j.envsci.2016.01.016.

Seitzinger, S.P., R.V Styles, E.W. Boyer, R.B. Alexander, G. Billen, R.W. Howarth, B. Mayer, and N. Van Breemen. 2002. Nitrogen retention in rivers: Model development and application to watersheds in the northeastern U.S.A. In *The Nitrogen Cycle at Regional to Global Scales*, ed. E. W. Boyer and R. W. Howarth, 57–58:199–237. Dordrecht: Springer Netherlands. https://doi.org/10.1007/978-94-017-3405-9_6.

Sin, Y., E. Lee, Y. Lee, and K. H. Shin. 2015. The river-estuarine continuum of nutrients and phytoplankton communities in an estuary physically divided by a sea dike. *Estuarine, Coastal and Shelf Science* 163. Elsevier Ltd: 279–289. https://doi.org/10.1016/j.ecss.2014.12.028.

Smith, V.H., and D.W. Schindler. 2009. Eutrophication science: Where do we go from here? *Trends in Ecology & Evolution* 24: 201–207. https://doi.org/10.1016/j.tree.2008.11.009.

Tank, J.L., E.J. Rosi-Marshall, M.A. Baker, and R.O. Hall. 2008. Are rivers just big streams? A pulse method to quantify nitrogen demand in a large river. *Ecology* 89: 2935–2945. https://doi.org/10.1890/07-1315.1.

They, N.H., A.M. Amado, and J.B. Cotner. 2017. Redfield ratios in inland waters: Higher biological control of C:N: P ratios in tropical semi-arid high water residence time lakes. *Frontiers in Microbiology*. https://doi.org/10.3389/fmicb.2017.01505.

Ward, G. H. 1997. Processes and trends of circulation within the Corpus Christi Bay National Estuary Program study area. Texas Natural Resource Conservation Commission.

Wickham, H. 2016. *ggplot2: Elegant Graphics for Data Analysis*. New York: Springer-Verlag.

Wollheim, W.M., C.J. Vörösmarty, B.J. Peterson, S.P. Seitzinger, and C.S. Hopkinson. 2006. Relationship between river size and nutrient removal. *Geophysical Research Letters* 33: L06410. https://doi.org/10.1029/2006GL025845.

Worm, B., E.B. Barbier, N. Beaumont, J.E. Duffy, C. Folke, B.S. Halpern, J.B.C. Jackson, et al. 2006. Impacts of biodiversity loss on ocean ecosystem services. *Science* 314: 787–790. https://doi.org/10.1126/science.1132294.

Xu, X., H. Wei, G. Barker, K. Holt, S. Julian, T. Light, S. Melton, et al. 2021. Tidal freshwater zones as hotspots for biogeochemical cycling: Sediment organic matter decomposition in the lower reaches of two south Texas rivers. *Estuaries and Coasts* 44: 722–733. https://doi.org/10.1007/s12237-020-00791-4.